

MBVI: Model-Based Value Initialization for Reinforcement Learning

¹Xubo Lyu ¹Site Li ²Seth Siriya ²Ye Pu ¹Mo Chen

¹School of Computing Science, Simon Fraser University, Canada

²Department of Electrical and Electronic Engineering, The University of Melbourne, Australia

{xlv, sitel}@sfu.ca, mochen@cs.sfu.ca,
ssiriya@student.unimelb.edu.au, ye.pu@unimelb.edu.au

Abstract: Model-free reinforcement learning (RL) is capable of learning control policies for high-dimensional, complex robotic tasks, but tends to be data inefficient. Model-based RL and optimal control have been proven to be much more data-efficient if an accurate model of the system and environment is known, but can be difficult to scale to expressive models for high-dimensional problems. In this paper, we propose a novel approach to alleviate data inefficiency of model-free RL by warm-starting the learning process using model-based solutions. We do so by initializing a high-dimensional value function via supervision from a low-dimensional value function obtained by applying model-based techniques on a low-dimensional problem featuring an approximate system model. Therefore, our approach exploits the model priors from a simplified problem space implicitly and avoids the direct use of high-dimensional, expressive models. We demonstrate our approach on two representative robotic learning tasks and observe significant improvements in performance and efficiency, and analyze our method empirically with a third task.

Keywords: Reinforcement Learning, Value Initialization, Optimal Control

1 Introduction

Model-free reinforcement learning (RL) has been successfully applied in games and robotics [1, 2] for solving complex, high-dimensional tasks. By mapping observations to actions via (deep) neural network approximators [3, 4], model-free RL allows the control policies to be learned directly from high-dimensional inputs. However, model-free RL often requires an impractically large number of trials to learn desired behaviours which is costly and unrealistic especially in the context of robotics. To address such sample efficiency challenge, prior model-free RL methods incorporate techniques such as curiosity-based exploration [5, 6], curriculum learning [7, 8], while model-based RL methods try to incorporate environment model information into policy learning [9, 10, 2].

Model-based methods learn and maintain a transition model of the domain environment online. Model-based RL achieves improved sample efficiency when it is able to learn a good model quickly [11, 12], but can perform poorly otherwise. Model-based RL is challenging in many high-dimensional robotic tasks especially when one aims to map sensor inputs directly to control actions, since the evolution of sensor inputs over time can be very difficult to model even using large, expressive neural networks [13, 14]. Such shortcomings can limit the model-based RL to relatively simple and low-dimensional tasks.

Optimal control has been widely used in various robotic applications [15, 16, 17, 18, 19]. It can be considered a classical method in contrast to more recent learning-based methods, and can provide solutions to many tasks without collecting any data from the environment, as long as an accurate system model is known. Optimal control lacks scalability to large-scale problems with high-dimensional state space especially when one aims to derive control policy from raw sensor input.

In this paper, we propose model-based value initialization (MBVI), a novel approach that improves data efficiency of model-free RL on high-dimensional problems by leveraging solutions from associated low-dimensional problems. This is accomplished by initializing the value function of the RL algorithm in a supervised fashion, where the supervision is obtained by solving a low-dimensional problem with either value iteration, a model-based RL technique or model predictive control, an optimal control technique.

We empirically evaluate our approach on two common mobile robotic tasks and obtain significant improvements in learning performance and efficiency. We choose Proximal Policy Optimization (PPO) [20] as a representative model-free algorithm to illustrate the effectiveness of our approach.

1.1 Related Work

Initializing or warm-starting reinforcement learning is a common technique to improve performance. To balance RL exploration against exploitation, optimistic value initialization [21, 22] has been proposed to initialize unseen states with higher values than are likely to be the true value. Imitation learning has also been often combined with RL; this can be done through policy initialization via learning from demonstrations [23, 24]. The demonstrations can come from humans or dynamical systems, and the initialized policy can be created through supervised learning or explicit programming [25, 26]. RL is used subsequently to fine-tune the policy parameters for self-improvement [27, 28]. Our method can be regarded as a specific way to initialize RL value function with system dynamics priors. Unlike many imitation-based policy initialization approaches, we propose to initialize a value function from optimal control based demonstrations.

Combining optimal control and RL has the potential to inherit the benefits of both techniques. In [29, 30], model predictive control (MPC) has been employed to either generate guided training data or provide trajectory optimization based supervision for RL to learn complex, high-dimensional policies. Within the curriculum RL framework, reachability theory has been applied to provide a more intuitive, accurate criterion for curriculum generation [31]. Recently, the authors of [32] presented an approach to shape the RL reward function by solving time-to-reach (TTR) problems. Our approach aims to improve sample efficiency by leveraging solutions lower-dimensional problems produced by optimal control to facilitate the learning of high-dimensional RL policies.

2 Preliminaries

2.1 RL Notations and Terminologies

Consider a Markov Decision Process (MDP) with agent and environment state S , a set of agent actions A , a probability of transition (at any time t) from state s to state s' under action a : $P_a(s, s') = \Pr(s_{t+1} = s' | s_t = s, a_t = a)$ and an immediate reward $r(s_t, a_t)$. In this paper, we simplify the reward function as $r(s_t)$ so that it only depends on current state s_t . To match notations of the approximate system dynamics discussed in section 3.1, we introduce a slight abuse of notation and write $s_{t+1} \sim f(s_t, a_t)$ to denote that s_{t+1} is drawn from the distribution $\Pr(s_{t+1} = s' | s_t = s, a_t = a)$. We use the phrase “full MDP model” to refer to the state transition $f(\cdot)$ in the target RL problem.

The policy $\pi(a|s)$ specifies the probability of action a that the agent will choose in state s . The trajectory τ is a sequence of states and actions in the environment $\tau = (s_0, a_0, s_1, a_1, \dots)$, and the discounted return is denoted as $R(\tau) = \sum_{t=0}^{\infty} \gamma^t r(s_t)$ which is the discounted sum of all rewards obtained by the agent. Here $\gamma \in [0, 1]$ denotes a discount factor to involve the effect of long-term reward. $R_t = \sum_{t'=t}^T \gamma^{t'-t} r(s_{t'})$ is reward-to-go which is the sum of discounted rewards after a point in a trajectory. We also denote on-policy value function as $V^\pi(s)$, which gives the expected return starting in state s and always acting according to policy π , and the advantage function as $A^\pi(s, a)$, which describes how much better or worse it is than other actions on average.

Given an MDP, RL aims to find a policy π to maximize the expected return $J(\pi) = \mathbb{E}_{\tau \sim \pi} [R(\tau)]$.

2.2 Actor Critic RL

Policy gradient methods maximize the expected return by repeatedly estimating its gradient with respect to policy parameters θ and use it to directly update the policy $\pi_\theta(a|s)$ via stochastic gradient ascent: $\theta_{k+1} = \theta_k + \alpha \nabla_\theta J(\pi_{\theta_k})$. Actor critic methods, as an important class of policy gradient methods, aim to obtain better policy gradient estimates by concurrently updating a policy $\pi(a|s)$ (actor) and a value function $V^\pi(s)$ (critic) corresponding to π . Intuitively, the critic is used to evaluate the actor and drive the actor’s policy parameters in the direction of performance improvement. In this paper, we assume that the policy gradient is given by the following expression [33]:

$$g = \nabla_\theta J(\pi_\theta) = \mathbb{E}_{\tau \sim \pi_\theta} \left[\sum_{t=0}^T \nabla_\theta \log \pi_\theta(a_t | s_t) \left(G_t^\lambda - V^\pi(s_t) \right) \right] \quad (1)$$

where G_t^λ is the TD(λ) return [34] which considers weighted average of n -step returns for $n = 1, 2, \dots, \infty$ using λ . Particularly, G_t^λ becomes Monte-Carlo return [35] $\sum_{l=0}^{\infty} \gamma^l r(s_{t+l})$ when $\lambda = 1$ and one-step TD return $r(s_t) + \gamma V^\pi(s_{t+1})$ when $\lambda = 0$.

In general, actor critic methods initialize value function V^π randomly and update it by constantly solving a nonlinear regression problem shown in Eq. (2), where \hat{R}_t is Monte-Carlo return from every s_t following policy π_θ and ϕ is value function parameters. In this paper, we take PPO algorithm with such default setting as a representative and denote it as a benchmark method in section 4.

$$\text{minimize}_\phi \sum_{t=1}^T \left\| V_\phi^\pi(s_t) - \hat{R}_t \right\|^2 \quad (2)$$

2.3 Baseline in Policy Gradient

In Eq. (1), $V^\pi(s_t)$ can be substituted by any function of the state $b(s_t)$, called the baseline, for the policy gradient estimate, potentially reducing variance without changing the expectation [36].

One common choice of baseline is the on-policy value function $V^\pi(s_t)$ that approximates the expected return, which provides the lowest variance [36]. Empirically, the choice $b(s_t) = V^\pi(s_t)$ results in more stable policy learning compared to other choices. However, this is not always good in many complex tasks especially when sufficient exploration is needed. In our method, we replace the online value function $V^\pi(\cdot)$ by a specialized, model-informed value function to significantly benefit on-policy learning even with very sparse reward.

2.4 Value Iteration

Value function V^π corresponding to any policy π can be computed by iteratively applying Bellman expectation backup [37] until it converges. In particular, we start with an arbitrary function V_0^π and recursively uses Eq. (3) to get the function for the $k + 1$ iteration V_{k+1}^π from the function for the k iteration V_k^π . Note that the choice of π is quite flexible considering the balance between RL exploration and exploitation. Unlike the greedy (optimal) policy used in classic value iteration, we instead use Boltzmann policy [38] in this paper to take policy stochasticity into account.

$$V_{k+1}(s) = \sum_{a \in A} \pi(a|s) (r(s, a) + \gamma \sum_{s' \in S} \mathcal{P}(s'|s, a) \cdot V_k(s')) \quad (3)$$

Value iteration method often applies in discrete and low-dimensional state space. This restricts its use on many complicated RL tasks despite the theoretical guarantee on the convergence to global optimality. However, by incorporating the value priors from low-dimensional problems into high-dimensional RL tasks in the manner of function initialization, our approach benefits the policy learning with significant improvement on data efficiency, as shown in section 3.

2.5 Model Predictive Control

Compared to model-free RL, model predictive control (MPC) uses a model of a system to predict the system’s future behaviour and optimize a given performance index, possibly subject to input and state constraints [39, 40]. More specifically, MPC repeatedly solves a constrained planning problem with a look-ahead horizon T at each time step t and only executes the first element of the control sequence obtained. Note that for most RL problems, one can define related MPC problems and solve it if the system model is known.

In this work, we take MPC solutions of a simplified, lower-dimensional problem involving a lower-dimensional system model, and map it to the value function of target high-dimensional RL task. More details are discussed in section 3.2.

3 Model-based Value Initialization

Before proceeding, we first introduce necessary notations and terminologies used in this section. The target RL problem we are solving that involves full MDP model $f(\cdot)$ is denoted as Ω . For every Ω , we denote its counterpart, a simplified, low-dimensional problem that involves a approximate, low-dimensional model $\tilde{f}(\cdot)$ as $\tilde{\Omega}$ (described in Section 3.1). Additionally, we denote the value function that is used in actor-critic algorithm for the problem Ω as $V_\phi(\cdot)$ and the policy function as $\pi_\theta(\cdot)$, with ϕ, θ representing function parameters. Correspondingly, the value function for $\tilde{\Omega}$ is denoted as $\tilde{V}(\cdot)$ (described in Sections 3.2, 3.3).

We now present our model-based value initialization¹ (MBVI) approach. Our algorithm starts with choosing an approximate system model $\tilde{f}(\cdot)$, which should be relatively low-dimensional but captures the key system behaviors of full MDP $f(\cdot)$ in the target RL problem Ω (Section 3.1). Then, we employ either model-based RL (value iteration) or optimal control (MPC) to solve the simplified problem $\tilde{\Omega}$ that features $\tilde{f}(\cdot)$ to collect training data $\mathcal{D} := \{(s_i, \tilde{V}(\tilde{s}_i))\}$ (Section 3.2). \mathcal{D} contains the mapping between states in Ω and approximate values in $\tilde{\Omega}$, and is used to train value function parameters ϕ_0 . With the initialized value function V_{ϕ_0} and randomly initialized policy π_{θ_0} , we begin updating θ_0 with any actor-critic RL algorithm. At each iteration k , we use the policy gradient \hat{g}_k obtained from online trajectories \mathcal{T}_k to update policy θ_k , and optionally update value function parameters ϕ_k based on a criterion described in Section 3.3. Algorithm 1 summarizes our method.

Algorithm 1 MBVI

- 1: Select an approximate model $\tilde{f}(\cdot)$ for the target RL problem Ω , and recognize a corresponding simplified problem $\tilde{\Omega}$ featuring $\tilde{f}(\cdot)$.
 - 2: Apply value iteration or MPC to $\tilde{\Omega}$ to collect training dataset $\mathcal{D} := \{(s_i, \tilde{V}(\tilde{s}_i))\}$.
 - 3: Initialize value function parameters ϕ_0 via supervised learning on \mathcal{D} . Initialize policy parameters θ_0 randomly.
 - 4: **for** $k = 0, 1, 2, \dots$ **do**
 - 5: Collect trajectories $\mathcal{T}_k = \{\tau_i | i = 0, 1, 2, \dots\}$ by running policy $\pi_k = \pi_{\theta_k}$ in target RL domain.
 - 6: Estimate rewards-to-go \hat{R}_t , advantage \hat{A}_t for every s_t and policy gradient \hat{g}_k using V_{ϕ_k} .
 - 7: Update policy $\theta_{k+1} = \theta_k + \alpha_k \hat{g}_k$
 - 8: Compute averaged Monte-Carlo return G_k^{MC} and value prediction $G_k^{V_\phi}$ using Eq. (8) (9).
 - 9: Update value function parameters ϕ based on Eq. (10) if $G_k^{MC} \geq G_k^{V_\phi}$, otherwise $\phi_{k+1} = \phi_k$.
 - 10: **end for**
-

3.1 Model Selection

“Model selection” refers to choosing an approximate, low-dimensional system model for the target RL task and compute value function based on it. The full MDP model $f(\cdot)$ is often inaccessible since it captures the evolution of high-dimensional state inputs including both sensor data and robot internal state. However, an approximate system model $\tilde{f}(\cdot)$ is often known and accessible. The tilde implies it is not necessary for $\tilde{f}(\cdot)$ to perfectly reflect the real state transitions $f(\cdot)$. In fact, $\tilde{f}(\cdot)$ should typically be lower-dimensional to allow for efficient value computation, while still capturing key robot physical dynamics.

The connection between the full MDP model and the approximate system model is formalized as follows. We assume that the approximate system state is a subset of the full MDP state s : $s = (\tilde{s}, \hat{s})$; \hat{s} denotes state components in the full MDP model that are not part of \tilde{s} . We assume that \tilde{s} evolves according to the following known model:

$$\dot{\tilde{s}}(t) = \tilde{f}(\tilde{s}(t), \tilde{a}(t)) \quad (4)$$

For example, in the simulated car example shown in section 4.1, the full state $s = (x, y, \theta, v, \omega, \dots, d_1, \dots, d_8)$ includes the position (x, y) , heading θ , speed v , turn rate ω , as well as eight laser range measurements d_1, \dots, d_8 that provide distances from nearby obstacles. As one can imagine, the evolution of s can be very difficult if $f(\cdot)$ is impossible to obtain, especially in a *a priori* unknown environment.

The state of the approximate system, denoted \tilde{s} , contains a subset of the internal states $(x, y, \theta, v, \omega)$, and evolves according to Eq. (4). In particular, for the simulated results in this paper, we choose the simple Dubins Car model to be the approximate system dynamics given in Eq. (5). As we will show, such simple dynamics are sufficient for improving data efficiency in model-free RL. With this choice, the remaining states are denoted $\hat{s} = (v, \omega, d_1, \dots, d_8)$.

$$\dot{\tilde{s}} = \begin{bmatrix} \dot{x} \\ \dot{y} \\ \dot{\theta} \end{bmatrix} = \begin{bmatrix} v \cos \theta \\ v \sin \theta \\ \omega \end{bmatrix} \quad (5)$$

$$\dot{\hat{s}} = \begin{bmatrix} \dot{x} \\ \dot{y} \\ \dot{\theta} \\ \dot{v} \\ \dot{\omega} \end{bmatrix} = \begin{bmatrix} v \cos \theta \\ v \sin \theta \\ \omega \\ \alpha_v \\ \alpha_\omega \end{bmatrix} \quad (6)$$

¹Code of this work is available at https://github.com/SFU-MARS/SL_optCtrl

It is worth noting that if a higher-fidelity model of the car is desired, one may also choose the following 5D ODE approximate system model (see appendix) instead, where we would have $\tilde{s} = (x, y, \theta, v, \omega)$, and $\tilde{s} = (d_1, \dots, d_8)$ in this case. In general, we may choose \tilde{s} such that a reasonable explicit, closed-form model $\tilde{f}(\cdot)$ can be derived. Such a model should capture the key features in the evolution of the robotic internal state.

The choice of an ODE model representing the real robot may be very flexible, depending on what behaviour one wishes to capture. In the 3D car example given in Eq. (5), we focus on modelling the position and heading of the car to be consistent with the goal. However, if speed and angular speed is deemed crucial for the task under consideration, one may also choose a more complex approximate system given by Eq. (6). To re-iterate, a good choice of approximate model is computationally tractable for the value function computation, and captures the system behaviours that are important for performing the desired task.

3.2 Training Data Generation

We generate training data $\{s_i, \tilde{V}(\tilde{s}_i)\}$ to train a value network $V_\phi(s)$ to be used as the critic in the RL method. The state s_i can be obtained by either directly sampling from the full MDP problem Ω or mapping from $\tilde{\Omega}$ to Ω . $\tilde{V}(\tilde{s}_i)$ is obtained by plugging in \tilde{s}_i into \tilde{V} , which can be computed using model-based methods such as value iteration or MPC. We now outline two examples.

Value iteration solution as ground truth We first consider the simple case, where the robotic system can be described via a sufficiently low-dimensional (normally no more than 4D) model. This is because value iteration is a dynamic programming-based method, whose computational complexity scales exponentially with system dimensionality.

For instance, a differential drive robot in this work can be modelled as a 3D system using Eq. (5). To apply value iteration on it, we apply discretization on the state $\tilde{s} = (x, y, \theta)$ and action $\tilde{a} = (v, \omega)$ space, and recursively calculate the value for each discrete state \tilde{s} following Eq. (3) until convergence. Then, to build the training dataset for $V_\phi(s)$, we randomly sample a large number of s_i , and compute their $\tilde{V}(\tilde{s}_i)$ accordingly. Thus, we obtain the training dataset $\{s_i, \tilde{V}(\tilde{s}_i)\}$.

MPC solution as ground truth Many complex robotic systems cannot be represented as models with a dimensionality low enough for tractable value iteration. A quadrotor is one example. Describing the dynamics of a planar quadrotor typically requires a 6D nonlinear dynamics, which is quite difficult to solve tractably using value iteration. In this case, we propose to use an MPC-aided, sampling-based approximation to estimate the value for such 6D state space (see appendix section C for a complete MPC problem formulation for this example).

Initial states are obtained by uniformly sampling from the 6D state space. Next, we utilize MPC to numerically solve the low-dimensional quadrotor problem given each of the initial states using the 6D approximate model (appendix section A) and specifying necessary domain constraints such as obstacles. This allows for collection of ample feasible and infeasible trajectories, with trajectories denoted as $\{\tilde{s}_i | i = 0, 1, 2, \dots, T\}$. We then take every state \tilde{s}_i in the trajectories and re-map it to s_i (obtaining corresponding sensor data for example), and compute $\tilde{V}(\tilde{s}_i)$ following Eq. (7), where $r(\cdot)$ is the reward function of the target RL problem Ω .

$$\begin{aligned} V(\tilde{s}_i) &= r(s_i) + \gamma V(\tilde{s}_{i+1}) \\ V(\tilde{s}_T) &= r(s_T) \end{aligned} \quad (7)$$

3.3 Value Network Training, Initialization and Update

We train the value network V_ϕ via supervised learning given the data set $\mathcal{D} = \{(s_i, \tilde{V}(\tilde{s}_i))\}$ collected from section 3.2. We choose mean squared error (MSE) as loss function. Once the value network is initialized using \mathcal{D} , we can easily integrate it as the critic into most actor-critic RL algorithms. This is in contrast to $V^\pi(s)$ in Eq. (1), which is normally initialized randomly. Therefore, the RL optimization starts as usual, except with the key system information implicitly involved.

$$G_k^{MC} = \frac{1}{|\mathcal{T}_k|} \sum_{\tau \in \mathcal{T}_k} \sum_{t=0}^T \gamma^t r(s_t) \quad (8) \quad G_k^{V_\phi} = \frac{1}{|\mathcal{T}_k|} \sum_{\tau \in \mathcal{T}_k} \sum_{t=0}^T V_{\phi_k}(s_t) \quad (9)$$

Additionally, we propose a criterion for optionally updating V_ϕ as follows. We compare the averaged Monte-Carlo return G_k^{MC} and averaged value prediction $G_k^{V_\phi}$ at each iteration k that are calculated

via Eq. (8) and (9), and update the value function using (10) if $G_k^{MC} \geq G_k^{V\phi}$.

$$\phi_{k+1} = \arg \min_{\phi} \frac{1}{|\mathcal{T}_k| T} \sum_{\tau \in \mathcal{T}_k} \sum_{t=0}^T (V_{\phi_k}(s_t) - \hat{R}_t)^2 \quad (10)$$

Such a criterion guarantees that the value function will get updated only if the roll-outs indicates perform favourably compared to the initialized value function suggests. This way, the value function updates do not deteriorate the value function as a result of an initially poorly performing policy.

4 Experimental Results

In this section, we compare the performance of the benchmark with our MBVI approach. The benchmark approach refers to using the original PPO algorithm with random value initialization and regular value update while the MBVI approach refers to the use of original PPO algorithm but with the value network initialized from an approximate system model, as described in section 3. Note that MBVI includes four variants: **VI-fixed**, **VI-updated**, **MPC-fixed** and **MPC-updated**, depending on the use of value iteration or MPC for value initialization. Additionally, “fixed” refers to value function staying the same as initialization all the time while “updated” means value function will be optionally updated via our novel criterion discussed in section 3.3. Without loss of generality and complexity, we employ sparse reward for all examples in this paper (see section B in appendix).

4.1 Differential Drive Car

We first apply our approach on a simulated TurtleBot navigating in an environment with multiple static obstacles. The goal of this task is to learn a control policy for the car to move from a starting area (green area in Fig. 1) to a specific goal area (yellow area in Fig. 1) following a collision-free trajectory. Particularly, the car starts with randomly-sampled positions and angles from the starting area $S_b = \{(x, y, \theta) | -0.5 \text{ m} \leq x \leq 0.5 \text{ m}; -3.5 \text{ m} \leq y \leq -2.5 \text{ m}; 0 \leq \theta \leq \pi\}$, and aims to arrive at the goal, which is defined as a 3D region $S_g = \{(x, y, \theta) | 3.7 \text{ m} \leq x \leq 4.3 \text{ m}; 3.7 \text{ m} \leq y \leq 4.3 \text{ m}; 0.45 \text{ rad} \leq \theta \leq 1.05 \text{ rad}\}$. The state and observation of this example are already discussed in section 3.1. The car moves by controlling the linear and angular velocities. Note that the robot is not aware of the environment in advance but needs to learn a control policy purely from trial and error. In our method, we initialize value function by applying value iteration or MPC on a lower-dimensional, approximate car system in Eq. (5) which only considers (x, y, θ) as state and angular velocity ω as control.

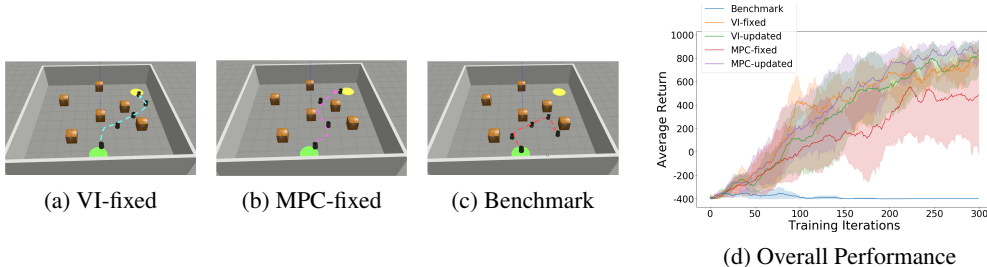


Figure 1: Simulated car trajectories at iteration 90 from (a) VI-fixed (b) MPC-fixed (c) Benchmark. Both variants of our approach successfully learn a collision-free, goal-reaching policy while benchmark method learns to stay conservatively. (d) Overall performance comparison on the car example.

Fig. 1d shows the learning progresses for different approaches. We take the averaged training return versus iterations as performance measurement. Results are summarized across 10 different trials. The curves show the mean return and the shaded area represents the standard deviation of 10 trials. As evident from Fig. 1d, all variants of our approach continue to improve as the learning progresses and eventually significantly outperforms the benchmark method. In terms of policy behaviours shown in Fig. 1a, 1b and 1c, our method can successfully learn collision-free paths despite the collisions in the earlier stage while the benchmark method only learns highly conservative behaviours such as staying around the same area after many failures.

In this example, value iteration is shown to be a better technique for value initialization compared to MPC. This makes sense since value iteration exhausts all possible state combinations of the low-dimensional system while MPC produces a finite set of locally optimal trajectories. With both value

iteration and MPC, allowing further value update further improves performance. This is especially true with MPC. This indicates the necessity of introducing an appropriate value update criterion. Intuitively, keeping a well-initialized value function fixed would be advantageous in preventing policy getting stuck in the early stage; however, eventually this fixed value function becomes somewhat detrimental later and can prevent further policy improvement.

4.2 Planar Quadrotor

In the second example, we select a planar quadrotor as a more complicated system to test our approach. The control of a quadrotor is usually considered challenging due to its under-actuated nature and the fact that its translational movement partly depends on its orientation. Therefore, the goal of this experiment is to validate that our model-based value initialization method still works well even on a highly dynamic and unstable system. “Planar” means the quadrotor is restricted to move in the vertical (x - z) plane by changing the pitch without affecting the roll and yaw.

The simulated setup is shown in Fig. 2 with starting region $S_b = \{(x, z, \psi) | 2.5 \text{ m} \leq x \leq 3.5 \text{ m}; 2.5 \text{ m} \leq z \leq 3.5 \text{ m}; -\pi/4 \leq \psi \leq \pi/4\}$ (green area) and goal region $S_g = \{(x, z, \psi) | 3.5 \text{ m} \leq x \leq 4.5 \text{ m}; 8.5 \text{ m} \leq z \leq 9.5 \text{ m}; 0 \leq \psi \leq \pi/3\}$. To initialize the value function, we choose the approximate system model (appendix section A) with a 6-dimensional internal state $\tilde{s} = (x, v_x, z, v_z, \psi, \omega)$, where x, z, ψ denote the planar positional coordinates and pitch angle, and v_x, v_z, ω denote their time derivatives respectively. The quadrotor receives full state $s = (x, v_x, z, v_z, \psi, \omega, d_1, \dots, d_8)$, which contains eight sensor readings extracted from the laser range finder for detecting obstacles, in addition to the internal state \tilde{s} . The quadrotor intends to learn a policy mapping from states and observations to thrusts that lead it to the goal.

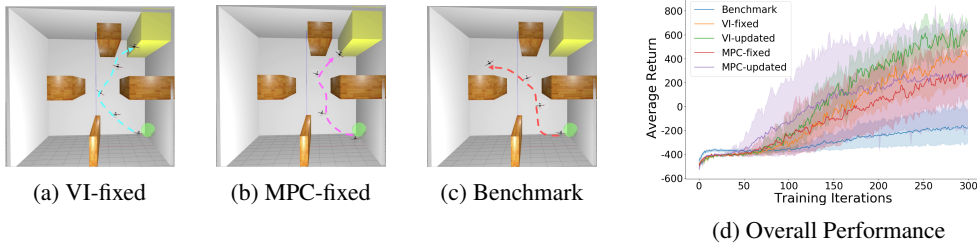


Figure 2: Simulated quadrotor trajectories from iteration 200 from (a) VI-fixed (b) MPC-fixed (c) Benchmark. Our approach learns to fly to the goal yet benchmark method keep failing in a undesired (upper-left) area and never recover. (d) Overall performance comparison on the quadrotor example.

Fig. 2d depicts the evaluation of our approach as well as the benchmark approach on the planar quadrotor, in a similar way as the car example. Compared to the car, the quadrotor is harder to control due to its unstable physical nature thereby leading to slightly inferior performance in general. Despite the computational complexity, we still apply value iteration on the 6D approximate state space to fully test our approach on complex systems. The average returns from the four variants of our approach start outperforming the benchmark after around 50 iterations. In contrast with MPC based technique, value iteration based initialization ends up with the best performance and much lower variance, indicating its notable advantage in giving accurate, robust value supervision. However, it is worth noting that the MPC based technique retains more scalability to relatively complex systems without losing too much learning performance.

The trajectories comparisons in Fig. 2 also highlight the efficacy of our approach. The benchmark method fails to find the correct path and gets stuck in an undesirable region. This is potentially because the benchmark method forces value function to be constantly updated towards policy return, and this can result in near-zero advantage estimate (see Eq. (1)) and restrain further policy update and exploration, which is especially unfavourable to an initially poorly performing policy. In contrast, the variants of our approach can avoid such issue by leveraging approximate model priors and the novel value update criterion. As a result, our method tractably and reliably learns a policy that smoothly and successfully reaches the goal.

5 Discussion: Policy Gradient Correctness

In this section, we investigate the correctness of policy gradient estimate in the learning process for a “Trap-Goal” environment to gain insight on why our method is able to improve learning. Additional

analysis on the advantage estimate and policy gradient variance can be found in appendix section D. Note that we take **VI-fixed** as a representative variant of our MBVI approach.

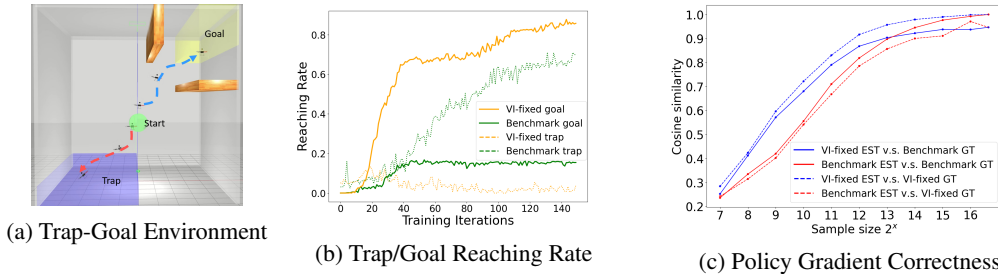


Figure 3: (a) Quadrotor trajectories in the Trap-Goal environment using MBVI method (blue dashed line) and benchmark (red dashed line). (b) The training performance of MBVI and benchmark in terms of goal and trap reaching rate. (c) Policy gradient estimate correctness comparison between MBVI method and benchmark.

To highlight the importance of correct gradient estimate in RL tasks, we purposely design an example (Fig. 3a) in which there is a goal (yellow area) and trap (purple area) that give positive but various rewards (+1000 for goal, +100 for trap) such that the correct policy gradient should drive the policy towards reaching the goal despite possible misleading gradients caused by the trap.

Fig. 3a depicts trajectories from executing policies learned from MBVI and benchmark methods. Under the same exploration strategy, the benchmark method leads to a trap-reaching policy (red dashed line) while our MBVI method learns the desired goal-reaching policy (blue dashed line). This result is also reflected in Fig. 3b where MBVI approach has an increasing goal-reaching rate as learning progresses while the benchmark method has an increasing trap-reaching rate.

Fig. 3c statistically illustrates the correctness comparison of policy gradient estimate between MBVI and benchmark, in terms of cosine similarity versus sample size. Particularly, we denote **benchmark GT** and **VI-fixed GT** as two types of policy gradient ground truths, which are computed by benchmark and MBVI methods following Eq. (1) over infinite (N_{\max}) samples² collected by running a fixed policy π . Correspondingly, with $N(N \leq N_{\max})$ samples, we obtain two types of policy gradient estimates named **benchmark EST** and **VI-fixed EST**. We then compute the cosine similarity between **benchmark EST/VI-fixed EST** and two ground truths respectively with multiple choices of N and plot the results in Fig. 3c. The result is averaged over 100 random selections of N samples. As evident from the figure, our approach (blue solid and dashed lines) always leads to more accurate gradient estimate with higher cosine similarity than the benchmark (in terms of gradient direction), regardless of sample size or ground truth type, especially at relatively low N .

6 Conclusion

We propose model-based value initialization, a novel approach to alleviate the data inefficiency of model-free RL by implicitly leveraging model priors. This is achieved by first solving a simplified, lower-dimensional version of the RL problem using model-based methods, which allows the use of known approximate system models. The value function obtained from this lower-dimensional solution is used to initialize the parameters of the full-dimensional value function in the original RL problem. The results show that our approach can accelerate learning by taking advantage of an inaccurate model yet still retains the flexibility of model-free RL methods. Our method is effective when explicit robotic system dynamics are accessible. Data efficiency can be greatly improved even with a low-dimensional, approximate system dynamics.

References

- [1] V. Mnih, K. Kavukcuoglu, D. Silver, A. Graves, I. Antonoglou, D. Wierstra, and M. Riedmiller. Playing atari with deep reinforcement learning. *arXiv preprint arXiv:1312.5602*, 2013.
- [2] N. O. Lambert, D. S. Drew, J. Yaconelli, S. Levine, R. Calandra, and K. S. Pister. Low-level control of a quadrotor with deep model-based reinforcement learning. *IEEE Robotics and Automation Letters*, 4(4):4224–4230, 2019.

²In practice, we select a relatively large number $N_{\max} = 102400$ instead of ∞ to compute the ground truth.

- [3] R. S. Sutton, D. A. McAllester, S. P. Singh, and Y. Mansour. Policy gradient methods for reinforcement learning with function approximation. In *Advances in neural information processing systems*, pages 1057–1063, 2000.
- [4] J. Schulman, S. Levine, P. Abbeel, M. Jordan, and P. Moritz. Trust region policy optimization. In *International conference on machine learning*, pages 1889–1897, 2015.
- [5] D. Pathak, P. Agrawal, A. A. Efros, and T. Darrell. Curiosity-driven exploration by self-supervised prediction. *2017 IEEE Conference on Computer Vision and Pattern Recognition Workshops (CVPRW)*, pages 488–489, 2017.
- [6] Y. Burda, H. A. Edwards, D. Pathak, A. J. Storkey, T. Darrell, and A. A. Efros. Large-scale study of curiosity-driven learning. *ArXiv*, abs/1808.04355, 2019.
- [7] Y. Bengio, J. Louradour, R. Collobert, and J. Weston. Curriculum learning. In *Proc. Annual Int. Conf. Machine Learning*, 2009.
- [8] C. Florensa, D. Held, M. Wulfmeier, and P. Abbeel. Reverse curriculum generation for reinforcement learning. *CoRR*, 2017. URL <http://arxiv.org/abs/1707.05300>.
- [9] T. Hester and P. Stone. Learning and using models. In M. Wiering and M. van Otterlo, editors, *Reinforcement Learning: State of the Art*. Springer Verlag, Berlin, Germany, 2011.
- [10] D. Silver, A. Huang, C. J. Maddison, A. Guez, L. Sifre, G. Van Den Driessche, J. Schrittwieser, I. Antonoglou, V. Panneershelvam, M. Lanctot, et al. Mastering the game of go with deep neural networks and tree search. *nature*, 529(7587):484, 2016.
- [11] A. Nagabandi, G. Kahn, R. S. Fearing, and S. Levine. Neural network dynamics for model-based deep reinforcement learning with model-free fine-tuning. *2018 IEEE International Conference on Robotics and Automation (ICRA)*, pages 7559–7566, 2018.
- [12] T. Kurutach, I. Clavera, Y. Duan, A. Tamar, and P. Abbeel. Model-ensemble trust-region policy optimization. In *International Conference on Learning Representations*, 2018. URL <https://openreview.net/forum?id=SJJinbWRZ>.
- [13] M. P. Deisenroth and C. E. Rasmussen. Reducing model bias in reinforcement learning. 2010.
- [14] E. Langlois, S. Zhang, G. Zhang, P. Abbeel, and J. Ba. Benchmarking model-based reinforcement learning. *arXiv preprint arXiv:1907.02057*, 2019.
- [15] S. Wang and K. Hauser. Realization of a real-time optimal control strategy to stabilize a falling humanoid robot with hand contact. In *2018 IEEE International Conference on Robotics and Automation (ICRA)*, pages 3092–3098, May 2018. doi:10.1109/ICRA.2018.8460500.
- [16] M. Chen and C. J. Tomlin. Hamilton–jacobi reachability: Some recent theoretical advances and applications in unmanned airspace management. *Annual Review of Control, Robotics, and Autonomous Systems*, 1:333–358, 2018.
- [17] M. Chen, Q. Hu, J. F. Fisac, K. Akametalu, C. Mackin, and C. J. Tomlin. Reachability-based safety and goal satisfaction of unmanned aerial platoons on air highways. *Journal of Guidance, Control, and Dynamics*, 40(6):1360–1373, 2017.
- [18] M. Chen, J. F. Fisac, S. Sastry, and C. J. Tomlin. Safe sequential path planning of multi-vehicle systems via double-obstacle hamilton-jacobi-isaacs variational inequality. In *2015 European Control Conference (ECC)*, pages 3304–3309. IEEE, 2015.
- [19] M. Chen, J. C. Shih, and C. J. Tomlin. Multi-vehicle collision avoidance via hamilton-jacobi reachability and mixed integer programming. In *2016 IEEE 55th Conference on Decision and Control (CDC)*, pages 1695–1700. IEEE, 2016.
- [20] J. Schulman, F. Wolski, P. Dhariwal, A. Radford, and O. Klimov. Proximal policy optimization algorithms. *CoRR*, abs/1707.06347, 2017.
- [21] I. Szita and A. Lőrincz. Optimistic initialization and greediness lead to polynomial time learning in factored mdps. In *Proceedings of the 26th Annual International Conference on Machine Learning, ICML '09*, page 1001–1008, New York, NY, USA, 2009. Association for Computing Machinery. ISBN 9781605585161. doi:10.1145/1553374.1553502. URL <https://doi.org/10.1145/1553374.1553502>.

- [22] M. C. Machado, S. Srinivasan, and M. Bowling. Domain-independent optimistic initialization for reinforcement learning. *ArXiv*, abs/1410.4604, 2015.
- [23] B. Kim, A.-m. Farahmand, J. Pineau, and D. Precup. Learning from limited demonstrations. In *Advances in Neural Information Processing Systems*, pages 2859–2867, 2013.
- [24] J. Chemali and A. Lazaric. Direct policy iteration with demonstrations. In *Twenty-Fourth International Joint Conference on Artificial Intelligence*, 2015.
- [25] J. Kober and J. Peters. Imitation and reinforcement learning. *IEEE Robotics & Automation Magazine*, 17(2):55–62, 2010.
- [26] J. Kober, K. Mülling, O. Krömer, C. H. Lampert, B. Schölkopf, and J. Peters. Movement templates for learning of hitting and batting. In *2010 IEEE International Conference on Robotics and Automation*, pages 853–858. IEEE, 2010.
- [27] J. Buchli, F. Stulp, E. Theodorou, and S. Schaal. Learning variable impedance control. *The International Journal of Robotics Research*, 30(7):820–833, 2011.
- [28] A. J. Ijspeert, J. Nakanishi, H. Hoffmann, P. Pastor, and S. Schaal. Dynamical movement primitives: learning attractor models for motor behaviors. *Neural computation*, 25(2):328–373, 2013.
- [29] T. Zhang, G. Kahn, S. Levine, and P. Abbeel. Learning deep control policies for autonomous aerial vehicles with mpc-guided policy search. In *2016 IEEE international conference on robotics and automation (ICRA)*, pages 528–535. IEEE, 2016.
- [30] G. Kahn, T. Zhang, S. Levine, and P. Abbeel. Plato: Policy learning using adaptive trajectory optimization. In *2017 IEEE International Conference on Robotics and Automation (ICRA)*, pages 3342–3349. IEEE, 2017.
- [31] B. Ivanovic, J. Harrison, A. Sharma, M. Chen, and M. Pavone. Barc: Backward reachability curriculum for robotic reinforcement learning. In *Proc. IEEE Int. Conf. Robotics and Automation*, 2019.
- [32] X. Lyu and M. Chen. Tr-based reward for reinforcement learning with implicit model priors. *arXiv preprint arXiv:1903.09762v2*, 2019.
- [33] J. Schulman, P. Moritz, S. Levine, M. I. Jordan, and P. Abbeel. High-dimensional continuous control using generalized advantage estimation. *CoRR*, abs/1506.02438, 2016.
- [34] R. S. Sutton. Learning to predict by the methods of temporal differences. *Machine learning*, 3(1):9–44, 1988.
- [35] R. S. Sutton and A. G. Barto. *Reinforcement learning: An introduction*. MIT press, 2018.
- [36] E. Greensmith, P. L. Bartlett, and J. Baxter. Variance reduction techniques for gradient estimates in reinforcement learning. *Journal of Machine Learning Research*, 5(Nov):1471–1530, 2004.
- [37] R. Bellman. Dynamic programming and stochastic control processes. *Information and control*, 1(3):228–239, 1958.
- [38] N. Cesa-Bianchi, C. Gentile, G. Lugosi, and G. Neu. Boltzmann exploration done right. In *Proceedings of the 31st International Conference on Neural Information Processing Systems, NIPS’17*, page 6287–6296, Red Hook, NY, USA, 2017. Curran Associates Inc. ISBN 9781510860964.
- [39] Y. Pu, M. N. Zeilinger, and C. N. Jones. Inexact fast alternating minimization algorithm for distributed model predictive control. In *53rd IEEE Conference on Decision and Control*, pages 5915–5921, 2014.
- [40] H. Hu, Y. Pu, M. Chen, and C. J. Tomlin. Plug and play distributed model predictive control for heavy duty vehicle platooning and interaction with passenger vehicles. In *2018 IEEE Conference on Decision and Control (CDC)*, pages 2803–2809, 2018.
- [41] X. Zhang, A. Liniger, and F. Borrelli. Optimization-based collision avoidance. *IEEE Transactions on Control Systems Technology*, 2020.

- [42] T. P. Lillicrap, J. J. Hunt, A. Pritzel, N. M. O. Heess, T. Erez, Y. Tassa, D. Silver, and D. Wierstra. Continuous control with deep reinforcement learning. *CoRR*, abs/1509.02971, 2016.
- [43] S. Fujimoto, H. Van Hoof, and D. Meger. Addressing function approximation error in actor-critic methods. *arXiv preprint arXiv:1802.09477*, 2018.

A Appendix

A System Dynamics of Planar Quadrotor

We use the following 6D ordinary differential equation to describe the evolution of the planar quadrotor:

$$\dot{s} = \begin{bmatrix} \dot{x} \\ \dot{v}_x \\ \dot{z} \\ \dot{v}_z \\ \dot{\psi} \\ \dot{\omega} \end{bmatrix} = \begin{bmatrix} -\frac{1}{m}C_D^v v_x + \frac{M_1}{m} \sin \psi + \frac{M_2}{m} \sin \psi \\ -\frac{1}{m}(mg + C_D^v v_z) + \frac{M_1}{m} \cos \psi + \frac{M_2}{m} \cos \psi \\ \omega \\ -\frac{1}{I_{yy}}C_D^\psi \omega + \frac{l}{I_{yy}}M_1 - \frac{l}{I_{yy}}M_2 \end{bmatrix}, \quad (11)$$

where the quadrotor's movement is controlled by two motor thrusts, M_1 and M_2 . The quadrotor has mass m , moment of inertia I_{yy} , and half-length l . Furthermore, g denotes the gravity acceleration, C_D^v the translation drag coefficient, and C_D^ψ the rotational drag coefficient.

B Reward Functions

We use Eq. (12) as the reward for the two examples in Section 4, where \mathbf{G} refers to the set of goal states, \mathbf{C} the set of collision states and \mathbf{I} the set of intermediate states which involves neither collision nor goal. Note that here s is the full MDP state, which includes both robotic internal states and sensor readings, for the target RL problem Ω .

Eq. (13) is used in Section 5 for the Trap-Goal environment. Here, \mathbf{Tr} represents the states in the trap area.

$$r(s) = \begin{cases} 0 & s \in \mathbf{I} \\ +1000 & s \in \mathbf{G} \\ -400 & s \in \mathbf{C} \end{cases} \quad (12) \quad r(s) = \begin{cases} 0 & s \in \mathbf{I} \\ +1000 & s \in \mathbf{G} \\ +100 & s \in \mathbf{Tr} \\ -400 & s \in \mathbf{C} \end{cases} \quad (13)$$

C Data Generation using MPC

C.1 General MPC Formulation

The goal of MPC for both examples is to generate trajectories from certain initial state to a desired goal region whilst avoidance obstacles. Using the point-mass base optimization-based collision avoidance approach Zhang et al. [41] the obstacle avoidance condition is:

$$\text{dist}(p, \mathbb{O}) > d_{min}, \quad (14)$$

where $\text{dist}(p, \mathbb{O}) := \min_t \{\|t\|_2 : (p+t) \cap \mathbb{O} \neq \emptyset\}$

Then, p is the position of the point-mass, $d_{min} \geq 0$ is a desired safety margin with the size of real robot taken into account, and \mathbb{O} denotes a polyhedral obstacle which is a convex compact set with non-empty relative interior, represented as

$$\mathbb{O} = \{p \in \mathbb{R}^n : Ap \leq b\}, \quad (15)$$

where $A \in \mathbb{R}^{l \times n}$, $b \in \mathbb{R}^l$, l is the number of sides of the obstacle and n is the number of position states. Since (14) is non-differentiable, we reformulate the condition into an equivalent differentiable condition: $\text{dist}(p, \mathbb{O}) > d_{min} \iff \exists \lambda \geq 0 : (Ap - b)^\top \lambda > d_{min}$, $\|A^\top \lambda\|_2 \leq 1$, where λ is the dual variable. We now formulate the general MPC optimization problem as follows:

$$\begin{aligned} \min_{\tilde{s}, \tilde{a}, \lambda} & \sum_{k=0}^{N-1} \left((p_k - p_{ref})^\top \gamma^{k+1} Q (p_k - p_{ref}) + \tilde{a}_k^\top R \tilde{a}_k \right) + (p_N - p_{ref})^\top \gamma^{N+1} Q (p_N - p_{ref}) \\ \text{s.t.} & \tilde{s}_0 = \tilde{s}_{initial} \\ & \tilde{s}_{k+1} = \tilde{s}_k + T_s \tilde{f}(\tilde{s}_k, \tilde{a}_k), \quad \tilde{a}_k \in \Delta, \quad \forall k \in \{0, \dots, N-1\} \\ & \tilde{s}_k \in \tilde{\mathcal{S}}, \quad \forall k \in \{0, \dots, N\} \\ & \tilde{s}_N \in \Gamma_3 \\ & \lambda_k^{(m)} \geq 0, \quad \left(A^{(m)} p_k - b^{(m)} \right)^\top \lambda_k^{(m)} > d_{min}, \quad \|A^{(m)\top} \lambda_k^{(m)}\|_2 \leq 1, \\ & \forall m \in \{1, \dots, M\}, \quad \forall k \in \{0, \dots, N\} \end{aligned} \quad (16)$$

To match the notations in the main paper, here we employ \tilde{s} and \tilde{a} as the state and action of a low-dimensional model (as in Eq. (11)) used in MPC. Tilde indicates it is an approximate model \tilde{f} in contrast to the full MDP model f of the target RL problem. Specifically, N is the horizon length, $\tilde{s} = [\tilde{s}_0, \dots, \tilde{s}_N]$ is all the states over the horizon, $\tilde{a} = [\tilde{a}_0, \dots, \tilde{a}_{N-1}]$ is the actions over the horizon, $\lambda = [\lambda_0^{(1)}, \dots, \lambda_0^{(M)}, \lambda_1^{(1)}, \dots, \lambda_N^{(M)}]$ is the dual variables associated with obstacles $\mathbb{O}^{(1)} \dots \mathbb{O}^{(M)}$ over the horizon, M is the number of obstacles, \tilde{s}_k is the states at time k , p_k is the positional states at time k , p_{ref} is the reference position, \tilde{a}_k is the control inputs at time step k , γ is the scaling factor for the position error, Q is the weight matrix for the position error, R is the weight matrix for the control effort, $\tilde{s}_{initial}$ is the initial state, T_s is the sampling period, \tilde{f} is the continuous-time system dynamics, Δ is the collection of possible control inputs, \tilde{S} is the state constraints, Γ_3 is the collection of goal states, and $A^{(m)} \in \mathbb{R}^{l \times n}$ and $b^{(m)} \in \mathbb{R}^l$ are the matrices that define the obstacle $\mathbb{O}^{(m)}$ based on (15).

C.2 Car Example MPC Formulation

In the car scenario, the continuous-time system dynamics \tilde{f} is:

$$\dot{\tilde{s}} = \tilde{f}(\tilde{s}, \tilde{a}) = \begin{bmatrix} \dot{x} \\ \dot{y} \\ \dot{\theta} \end{bmatrix} = \begin{bmatrix} v \cos(\theta) \\ v \sin(\theta) \\ \omega \end{bmatrix} \quad (17)$$

where $\tilde{s} = [x, y, \theta]^\top$ and $\tilde{a} = [v, \omega]^\top$. In the optimization problem we have $N = 80$, $p = [x, y]^\top$, $p_{ref} = [3.5, 3.5]^\top$, $\gamma = 1.1$, $Q = \text{diag}([10, 10]^\top)$, $R = \text{diag}([1, 1]^\top)$, $T_s = 0.05$, $\Delta = \{[v, \omega]^\top : -2 \leq v \leq 2, -2 \leq \omega \leq 2\}$, $\tilde{S} = \{[x, y, \theta]^\top : -4.723 \leq x \leq 4.723, -4.723 \leq y \leq 4.723, -\infty \leq \theta \leq \infty\}$, $\Gamma_3 = \{[x, y, \theta]^\top : \|[x, y]^\top - [3.5, 3.5]^\top\|_2 \leq 1, \cos(\theta - 0.75) \leq 0.3\}$, $d_{min} = 0.277$ and $M = 6$. The matrices for specifying obstacles $\mathbb{O}^{(1)} \dots \mathbb{O}^{(6)}$ are:

$$A^{(m)} = \begin{bmatrix} -1 & 0 \\ 1 & 0 \\ 0 & -1 \\ 0 & 1 \end{bmatrix}, \quad \forall m \in \{1, \dots, M\} \quad (18)$$

$$b^{(1)} = \begin{bmatrix} 0.35 \\ 0.35 \\ 0.35 \\ 0.35 \end{bmatrix}, b^{(2)} = \begin{bmatrix} -2.65 \\ 3.35 \\ 1.35 \\ -0.65 \end{bmatrix}, b^{(3)} = \begin{bmatrix} -1.65 \\ 2.35 \\ -0.65 \\ 1.35 \end{bmatrix}, b^{(4)} = \begin{bmatrix} 2.35 \\ -1.65 \\ 2.35 \\ -1.65 \end{bmatrix}, b^{(5)} = \begin{bmatrix} 0.35 \\ 0.35 \\ -3.65 \\ 4.35 \end{bmatrix}, b^{(6)} = \begin{bmatrix} 3.35 \\ -2.65 \\ -1.65 \\ 2.35 \end{bmatrix} \quad (19)$$

C.3 Quadrotor Example MPC Formulation

In the quadrotor scenario, the continuous-time system dynamics \tilde{f} is denoted as Eq. (11). In the optimization problem we have $N = 140$, $p = [x, z]^\top$, $p_{ref} = [4, 9]^\top$, $\gamma = 1.1$, $Q = \text{diag}([10000, 10000]^\top)$, $R = \text{diag}([1, 1]^\top)$, $T_s = 0.05$, $\Delta = \{[M_1, M_2]^\top : 5 \leq M_1 \leq 11, 5 \leq M_2 \leq 11\}$, $\tilde{S} = \{[x, v_x, z, v_z, \phi, \omega]^\top : -4.75 \leq x \leq 4.75, 0.25 \leq z \leq 9.75, -\pi/2 \leq \phi \leq \pi/2\}$, $\Gamma_3 = \{[x, z, \phi] : 3 \leq x \leq 5, 8 \leq z \leq 10, -\pi/3 \leq \phi \leq \pi/3\}$, $d_{min} = 0.1$ and $M = 4$. In the quadrotor scenario, $A^{(m)}$ is the same as the car scenario in (18). However, $b^{(1)}, \dots, b^{(4)}$ are:

$$b^{(1)} = \begin{bmatrix} 3.25 \\ -0.75 \\ -3.75 \\ 6.25 \end{bmatrix}, b^{(2)} = \begin{bmatrix} 1.25 \\ 1.25 \\ -7.5 \\ 9.5 \end{bmatrix}, b^{(3)} = \begin{bmatrix} -1.75 \\ 5.75 \\ -3.75 \\ 6.25 \end{bmatrix}, b^{(4)} = \begin{bmatrix} 0.75 \\ 0.75 \\ 0.5 \\ 2.5 \end{bmatrix}. \quad (20)$$

D More Discussions

D.1 Correctness of Policy Gradient Estimates

Following the procedure in Section 5, we now further investigate the correctness of gradient estimates in the Trap-Goal environment. We take policies at certain iterations in the earlier learning stage and employ these policies to collect sample transitions from the Trap-Goal environment. Particularly, we denote $\pi_G^{20}, \pi_G^{40}, \pi_G^{60}$ as polices belong to the goal-reaching trial at iteration 20, 40, 60; $\pi_{Tr}^{20}, \pi_{Tr}^{40}, \pi_{Tr}^{60}$ as polices belong to the trap-reaching trial at iteration 20, 40, 60.

We first take Fig. 4a, 4b and 4c as a group to analyze the results since they are all using trap-reaching policies. In the three sub-figures, MBVI approach always provide completely distinct gradient estimates from benchmark regardless of sample size or ground truth type (comparing blue, solid line to red, solid line, or blue, dashed line to red, dashed line). This suggests that MBVI is capable of distinguishing the wrong policy optimization direction in the Trap-Goal environment.

On the other hand, Fig. 4d, 4e and 4f show the cosine similarity for different sample sizes with the samples collected from goal-reaching policies. In this case, MBVI and the benchmark method both give consistent trends of gradient estimates. However, even in this case, our MBVI approach still provides more accurate gradient estimates than benchmark (blue solid and dashed lines are mostly above red solid and dashed lines respectively), especially at relatively lower sample sizes.

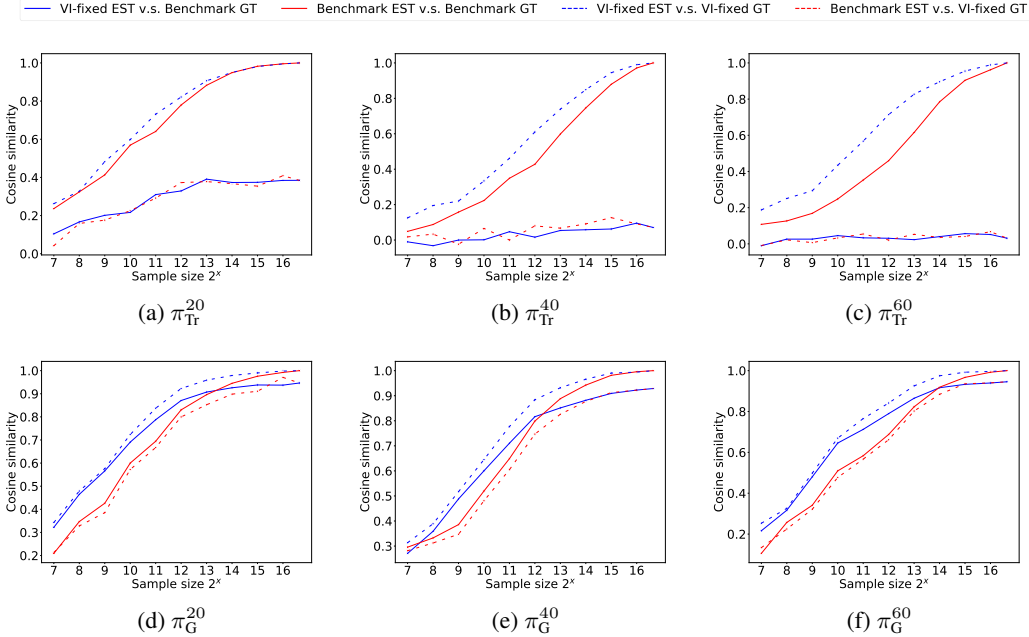


Figure 4: Policy gradient estimate correctness comparison between MBVI method and benchmark under multiple policies. We take (a), (b), (c) as a group, and (d), (e), (f) as another group to analyze. In each sub-figure, blue lines (solid or dashed) represent MBVI-based gradient estimate with regard to different types of ground truth while red lines (solid or dashed) represent benchmark method. A good comparison principle would be “blue solid v.s. red solid” or “blue dashed v.s. red dashed”.

D.2 Advantage Estimates

We also investigate the advantage estimates to empirically show the efficacy of MBVI algorithm. The advantage function $A^\pi(s, a)$ measures how much better an action a is than others on average, and has been extensively used in policy gradient algorithms to drive the policy update. In this paper, we assume the advantage is defined by $A^\pi(s, a) = G_t^\lambda - V^\pi(s_t)$ as shown in Eq. (1).

Fig. 5a shows the advantage estimates comparison between MBVI and the benchmark approach. The total number of training iterations are 150 and we take an average of advantage estimates every 10 iterations. It is clearly observed that MBVI approach maintains a relatively larger range of advantage estimates over the entire learning process. In contrast, the advantage estimates of the benchmark method gradually shrink to a very narrow range around zero. This may indicate that MBVI involves more exploration thus more likely to escape local optima. On the other hand, as we already observed in the Fig. 1c, benchmark method can often get stuck in an undesired area for a long time due to the negligible advantage estimates.

D.3 Variance of Policy Gradient Estimates

We also conduct empirical analysis on the variance of gradient estimates. More specifically, at each training iteration, we collect K^3 samples with each of them denoted as $D_i = (s_i, a_i, r_i, s_{i+1})$ using

³We use $K = 1024$ at each training iteration

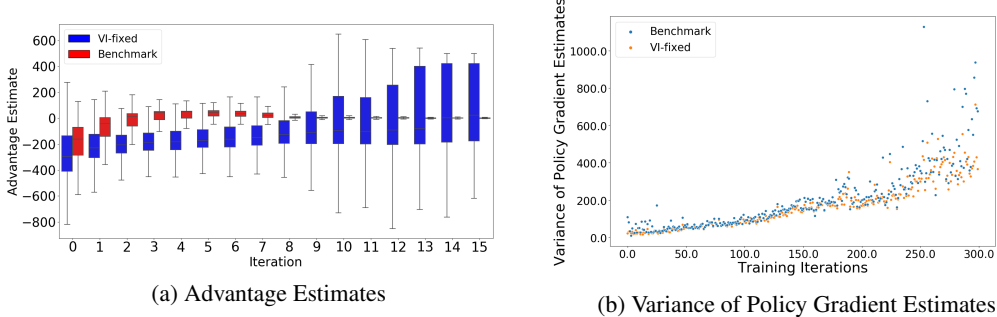


Figure 5: **(a)** Advantage estimates versus training iterations using MBVI and benchmark. Larger colored box refers to wider range of advantage estimates. **(b)** Policy gradient variance computed via MBVI and benchmark. Each dot corresponds to the magnitude of variance at certain iteration.

MBVI and benchmark methods respectively and calculate K policy gradients $\nabla_{\theta} J(\theta|D_i)$ based on each sample. Then we compute the largest singular value of co-variance matrix of each set of gradients $\{\nabla_{\theta} J(\theta|D_i) \mid i \in \{0, 1, \dots, K-1\}\}$.

Fig. 5b shows the gradient variance magnitude versus training iterations. MBVI (orange dots) and benchmark (blue dots) approaches share comparable variance of gradient estimates over the entire training process, which empirically indicates that MBVI maintains similar variance magnitude in its gradient estimates compared to the benchmark.

E Results on Q-learning based Algorithm

In contrast to direct policy gradient based methods (like PPO), Q-learning based methods are another important type of model-free RL algorithms. Deep Deterministic Policy Gradient (DDPG) algorithm is a well-known example. Unlike PPO which directly executes policy gradient optimization, DDPG first learns an on-policy Q function $Q^{\pi}(s, a)$ and then derives a policy based on $Q^{\pi}(s, a)$ Lillicrap et al. [42].

We test our MBVI algorithm on a refined DDPG algorithm (known as TD3 Fujimoto et al. [43]) to demonstrate its compatibility and efficacy on different types of model-free RL algorithms.

E.1 Important Procedure of DDPG Algorithm

In DDPG, the Q function $Q^{\pi}(s, a)$ is often represented by a nonlinear function approximator (e.g. neural network) with parameters ϕ , denoted as $Q_{\phi}^{\pi}(s, a)$. Here we simplify $Q_{\phi}^{\pi}(s, a)$ to $Q_{\phi}(s, a)$ for conciseness. In addition, a Q target function $Q_{\phi_{\text{targ}}}(s, a)$ is introduced in order to alleviate the optimization instability [42]. At each iteration, the Q target function $Q_{\phi_{\text{targ}}}(s, a)$ is also responsible for providing the Q function approximation target $y(r, s', d)$:

$$y(r, s', d) = r(s) + \gamma(1-d)Q_{\phi_{\text{targ}}}(s', \mu_{\theta_{\text{targ}}}(s')) \quad (21)$$

where $\mu_{\theta_{\text{targ}}}$ is the parameterized target policy. Then Q function $Q_{\phi}(s, a)$ is updated towards $y(r, s', d)$ by one-step gradient descent using Eq. (22) where \mathcal{B} is a batch of transition data sampled from original RL problem Ω :

$$\phi \leftarrow \phi - \alpha \nabla_{\phi} \frac{1}{|\mathcal{B}|} \sum_{(s,a,r,s',d) \in \mathcal{B}} (Q_{\phi}(s, a) - y(r, s', d))^2 \quad (22)$$

The policy μ_{θ} is updated subsequently via one-step gradient ascent towards $Q_{\phi}(s, a)$ via:

$$\theta \leftarrow \theta + \beta \nabla_{\theta} \frac{1}{|\mathcal{B}|} \sum_{s \in \mathcal{B}} Q_{\phi}(s, \mu_{\theta}(s)) \quad (23)$$

α and β are step sizes. The Q target $Q_{\phi_{\text{targ}}}(s, a)$ and policy target $\mu_{\theta_{\text{targ}}}$ then need to be updated in certain way such as polyak averaging:

$$\begin{aligned} \phi_{\text{targ}} &\leftarrow \rho \phi_{\text{targ}} + (1-\rho)\phi \\ \theta_{\text{targ}} &\leftarrow \rho \theta_{\text{targ}} + (1-\rho)\theta \end{aligned} \quad (24)$$

E.2 MBVI-based DDPG Algorithm

We take “VI-fixed” as the representative variant of our MBVI algorithm and integrate it into DDPG via the following two steps:

1. Use model-based value initialization $V_{\text{init}}(s)$ and one-step simulation to replace $Q_{\phi_{\text{target}}}(s, a)$ in Eq. (21), where the one-step simulation is shown as Eq. (25) assuming a deterministic full MDP model.

$$Q_{\phi_{\text{target}}}(s, a) = r(s) + \gamma V_{\text{init}}(s') \quad (25)$$

2. Disable the update of $Q_{\phi_{\text{target}}}(s, a)$ in Eq. (24).

Particularly in TD3 algorithm, there are two Q target functions: $Q_{\phi_{\text{target},1}}(s, a)$ and $Q_{\phi_{\text{target},2}}(s, a)$, and $y(r, s', d)$ is computed by:

$$y(r, s', d) = r(s) + \gamma(1 - d) \min_{i=1,2} Q_{\phi_{\text{target},i}}(s', a'(s')) \quad (26)$$

With MBVI, we simply use $V_{\text{init}}(s)$ and Eq. (25) to replace both Q target functions and disable the update of $Q_{\phi_{\text{target},1}}(s, a)$ and $Q_{\phi_{\text{target},2}}(s, a)$.

Fig. 6 illustrates how the learning progresses with MBVI-based and benchmark TD3 algorithms on the two robotic problems in Section 4. Note that here benchmark refers to the original TD3 algorithm with random initialized Q target function and regular Q target update. MBVI refers to a new TD3 algorithm that involves MBVI refinement described in this section. As evident from Fig. 6, MBVI continues to improve the policy with tolerable variance, and outperforms benchmark at around 50 iterations on both examples. For the quadrotor case, even though benchmark method eventually improves (at around 280 iteration), it lags behind MBVI and shows poor data efficiency.

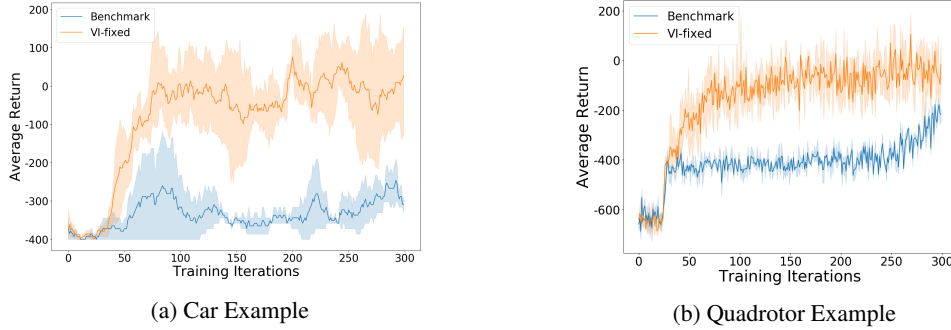


Figure 6: Overall learning performance comparison using MBVI-based and benchmark TD3 algorithms on two robotic examples. We take the averaged training return versus training iterations as performance measurement. Results are summarized across 5 different trials. The curves show the mean return and the shaded area represents the standard deviation of 5 trials.